ResearchGate

See discussions, stats, and author profiles for this publication at: https://www.researchgate.net/publication/7562856

Characterization of Freshwater Natural Aquatic Colloids by Atomic Force Microscopy (AFM)

ARTICLE *in* ENVIRONMENTAL SCIENCE AND TECHNOLOGY · OCTOBER 2005

Impact Factor: 5.33 · DOI: 10.1021/es050386j · Source: PubMed

CITATIONS
53

READS
61

3 AUTHORS, INCLUDING:

Christopher T Gibson
Flinders University
67 PUBLICATIONS **903** CITATIONS

SEE PROFILE

Available from: Christopher T Gibson
Retrieved on: 03 February 2016

Characterization of Freshwater Natural Aquatic Colloids by Atomic Force Microscopy (AFM)

J. R. LEAD,* D. MUIRHEAD, AND C. T. GIBSON

School of Geography, Earth and Environmental Science, University of Birmingham, Birmingham, B15 2TT, United Kingdom

Atomic force microscopy (AFM) has been used to image and quantify riverine colloids in a quantitative and relatively nonperturbing manner. Three main classes of material have been imaged including fibrils (about 10 nm in diameter and 100 nm or more in length), discrete, near-spherical, small colloids primarily below 30−50 nm in diameter, and a surface film, of at least several nanometers thickness, which coats the entire mica surface within 30 min of exposure to river water. Colloid structure was found to vary as a function of pH, particularly at high pH. Substantially different structures were observed at high pH values, with the loss of the near-spherical colloids possibly due to rearrangement and aggregation. In addition, film thicknesses of up to 100 nm were estimated on the silicon nitride AFM cantilever after 30 h of deposition in the same water (unperturbed and size fractionated). The observation of these surface films has important implications for understanding the mechanisms by which colloids might bind trace elements. In particular, development of surface coatings implies that binding of pollutants (at least initial surface binding) may be dominated by adsorbed surface layers.

Introduction

Natural aquatic colloids are complex mixtures of different physical, chemical, and biological phases defined as solid-phase material with one dimension less than 1 μm (*1*), although this definition is, in practice, usually operational and based on filtration (*2*). Other definitions, based on thermodynamic or environmental processes (*3*, *4*), have also been proposed. Colloids are composed of biological cells, organic material, and inorganic material, and there is increasing evidence that these components are held together in close, but easily perturbed, association (*5*, *6*).

Aquatic colloids have important effects on trace element fate and behavior, including impacts on their chemical behavior, their transport in surface waters and in groundwaters (*2*), and their bioavailability and toxicity through mechanisms such as alteration of cell surface charge and permeability. However, little information regarding the impacts of colloids on biouptake is available (*7*). Recent studies have implicated colloids in both enhanced and retarded biouptake and in altering trace element uptake and loss rates to organisms (*8*, *9*).

It is increasingly acknowledged that accurate understanding of the morphology, composition, and structure of these colloids on a single-particle basis is essential in understanding their role in the environment (*5*, *10*, *11*), in a manner analogous to the structure−function relationship of biological macromolecules. However, due to the profound complexity of colloidal structure and the limitations of analytical procedures, their structure and function is still poorly understood. This is especially the case for the very fine fractions of colloids (nanoparticles, <ca. 100 nm), with their low mass concentrations and unstable nature (*12*). These small colloids are of particular importance because they can potentially sorb large amounts of trace elements.

Increasingly, a range of different methodologies are becoming available for the nonperturbing and quantitative determination of colloid structure including transmission electron microscopy (TEM) (*13*), environmental scanning electron microscopy (ESEM) (*14*, *15*), fluorescence correlation spectroscopy (FCS) (*16*), and laser-induced breakdown spectroscopy (LIBD) (*17*). The study reported here uses the technique of atomic force microscopy (AFM) to probe quantitatively and with minimal perturbation the fine colloids present in an urban catchment. AFM has previously been used to study extracted humic substances (*18*, *19*) and marine polysaccharides (*10*), although always after substantial pretreatment in the laboratory by chemical extraction, filtration, and lyophilisation. In addition, the method has been used to qualitatively show the structure of groundwater colloids (*20*) and to investigate weathering rates and biofilm formation in an Antarctic stream using AFM (*21*). In addition, in force mode AFM has been used to probe the interactions between extracted humic substances (HS) or natural aquatic colloids and iron oxide surfaces (*22*−*24*). Previously, in our laboratories, the authors have performed initial scoping studies to characterize unperturbed samples taken directly from this urban water (*5*) and from a pristine glacier with minimal pretreatment (*25*). This paper reports one of the few studies to quantitatively probe the structures of small colloids from relatively nonperturbed aquatic samples, including an investigation of the effects of sample pH.

Methodology

Analysis of AFM Images and Transects. *Sampling and Preparation*. Samples were taken from four sites within a major U.K. conurbation (Birmingham, West Midlands) in both April and August of 2003. The first three samples were tributaries of the River Tame: the Ford Brook (site 1, Ordinance Survey ref 402650, 301900), the Oldbury Arms (site 2, OS ref 399200, 294300), and the Wolverhampton Arm (site 3, OS ref 398950, 297925). The fourth site was the River Tame (OS ref 401575, 295450), immediately after the confluence of the tributaries. Further details on the nature of the sampling sites can be found in ref 26 and references therein. Measurement of water pH, conductivity, temperature, and dissolved oxygen were also performed on the waters when sampling was performed. Conductivity was ca. 0.01 S, pH was ca. 7.0−7.5, and the temperature was ca. 10 °C for all samples. Dissolved oxygen near the surface was generally less than 100 % saturation, and usually about 60−80 %.

Sampling was performed on-site, following established procedures to ensure minimal perturbation of the sampling (*5*, *25*). All plastic ware was cleaned thoroughly in dilute acid (1 % HNO_3), 0.1 M $CaCl_2$, and pure water (R = 18.2 Ω cm) and rinsed with river water prior to sample collection. The washings were discarded. Samples were taken in 50 mL low-density polyethylene (LDPE) bottles taking care to prevent contamination and mixing. The bottles were left within larger containers filled with river water to ensure minimal tem-

* Corresponding author phone: (+44) 121 414 8147; fax: (+44) 121 414 5528; e-mail: j.r.lead@bham.ac.uk.

perature change. Freshly cleaved mica slides were inserted vertically into the sample, immediately after sampling, and left for 30 min on-site, before withdrawal. The mica slides were rinsed in pure water for 30 s, air-dried, and covered but left open to the air, to allow partial drying but prevent further deposition of atmospheric particles. For some sampling occasions, two samples were taken in order to investigate the effect of pretreatment through sedimentation. A second sample was taken and placed in a 1 L polythene container and left for 2 h at the ambient river water temperature to allow sedimentation of the large particles (>ca. 1 μm). From the 1 L sample, the top 2 cm was removed by pipet carefully. This collected subfraction was placed in a 50 mL LDPE bottle. A mica slide was placed in this fraction for 30 min as described above. The sedimentation procedure has previously been shown to remove the majority of large particles while leaving the colloidal fraction (*27*). In the second set of samples (August, 2003), similar sampling strategies were employed. In addition, the effect of pH was observed by the addition of either dilute NaOH or HNO_3. Similar imaging was performed on all samples. Colloids on the mica slides were relatively stable with no changes observed in images over at least 2 weeks. All AFM analysis was performed within 7 days of sampling.

Analysis. AFM images were obtained using a Digital Instruments Dimension 3100 in tapping mode, using a Si_3N_4 tip with a spring constant of 49 N m^{-1}. Tapping mode is recommended for soft material because of the reduction in lateral and vertical forces which may cause sample movement and deformation. Measurements of height and width were determined by recording changes in amplitude of the oscillating tip as it was scanned across the mica surface. Samples were analyzed at 20 °C and a relative humidity of 50−60 %, which leaves the samples with a small hydration layer, helping to maintain structure (*28*).

Images were analyzed quantitatively for surface film coverage, size distributions, and polydispersity (data on the latter two are given in the Supporting Information). AFM lateral dimensions are overestimates of size in colloids of this range, because the radius of curvature of the AFM tip is in the range of the colloid diameter (*18*). Therefore, AFM heights are used as estimates of diameter (see the Supporting Information), although with nonspherical natural colloids this height estimation is also subject to uncertainty. Use of the colloid height and the radius of curvature of the tip allowed the estimation of corrected lateral dimensions (*18*), although we acknowledge the uncertainties involved in this calculation. To estimate the possible effect of the tip dimensions we assumed the radius of curvature to be either 10 or 50 nm. These sizes were representative of a new, ideal tip and a usable tip, but after slight wear and tear due to previous measurement, respectively. These are not measured values but assumed in order to estimate the possible effects of tip dimensions on the correction of lateral dimensions.

Mass Deposited on AFM Cantilevers. Further samples were taken on October 5, 2004 from the same location and fractionated at 1 μm by split-flow thin cell (SPLITT) analysis, used as a relatively nonperturbing alternative to filtration (*29*). AFM cantilevers (DNP silicon nitride, V-shaped contact mode with a nominal spring constant of 0.06 N m^{-1}) were inserted into each of two sample types (original water and less than 1 μm) for 30 h in duplicate. Prior to insertion and after insertion the resonance frequency of each tip was measured with at least five measurements made in each sample. Similar measurements were performed in high-purity deionized water.

Added mass on the cantilever can be calculated from eq 1

$$M = k(\nu_1^{-2} - \nu_2^{-2})/(2\pi)^2 \quad (1)$$

where M is the added mass, k is the spring constant of the cantilever, ν_1 is the resonant frequency in air after immersion, and ν_2 is the resonant frequency in air before immersion. The added mass, M, can also be given by the following equation

$$M = nA\rho t \quad (2)$$

where n is a correction factor required since the cantilever is anchored at one end. The factor n depends on the geometry of the cantilever but can be obtained from published data (*30*). A is the surface area of the cantilever, ρ is the density of the material deposited onto the lever, and t is the thickness of this material (surface film thickness). Therefore, by substituting eq 2 into eq 1 we can find an expression for t which is as follows:

$$t = k(\nu_1^{-2} - \nu_2^{-2})/[nA\rho(2\pi)^2] \quad (3)$$

The surface area was determined by optical microscopy as 1.6×10^{-8} m^2, the correction factor n was 0.18 for these cantilevers, and a density of 1500 kg m^{-3} was assumed, which is reasonable for the aquatic colloids used.

Results and Discussion

Potential Uncertainty and Bias. Extreme care was taken in all aspects of the sampling and analysis, due to the known difficulties of determining colloidal structure. However, as with all methodologies, there are a number of potential uncertainties and errors. In the interests of clarity these need to be discussed in relation to the inherent bias and limitations of the method used. First, these images were taken under ambient humidity, as has been performed elsewhere (*18*, *25*). However, other studies have performed imaging under liquid water (*20*). At present, it is unclear which procedure produces the most satisfactory results, i.e., most similar to the in situ colloids, and a rigorous comparison on standards and "real" colloids under both conditions is urgently required. A priori, imaging under liquid water appears to provide ideal experimental conditions. However, atmospheric humidity retains colloid-bound water, helping to maintain structure (*28*), and AFM tips exposed to organic matter in solution soon become coated in the organic matter (*20*), potentially affecting the veracity of the images. This is also a possibility in imaging after air-drying. In the absence of a proven methodology, we have here opted to image at conditions of ambient humidity (relative humidity ca. 50 %). Second, the sampling procedure will likely result in bias toward the smaller, most diffusive colloids (*5*, *18*) although large colloids and particles may also be imaged (*10*, *21*, *25*). However, this ability to measure the fine (nanoparticle) fraction is one of the strengths of the AFM, but the greatest information content will be extracted when AFM is used with other techniques, as we propose to do in future studies. Third, the AFM will only measure those colloids which bind relatively strongly to the substrate (mica) surfaces.

Comparisons between TEM and AFM using different preparation methods have indicated similar morphologies in previous studies (*5*, *31*), and our AFM images correlate well with TEM images observed elsewhere (*32*) when imaging colloids from different waters, giving confidence in the observations reported here. However, imaging of Suwannee River humic acid (SRHA) in our laboratories by AFM and ESEM under identical conditions (*5*, *14*) has shown essentially different structures, indicating different "analytical windows" due to the different modes of operation and resolutions of the techniques. For instance, while ESEM measures lateral dimensions and has a resolution of ca. 30 nm, AFM measures heights and has a resolution substantially below 1 nm. When

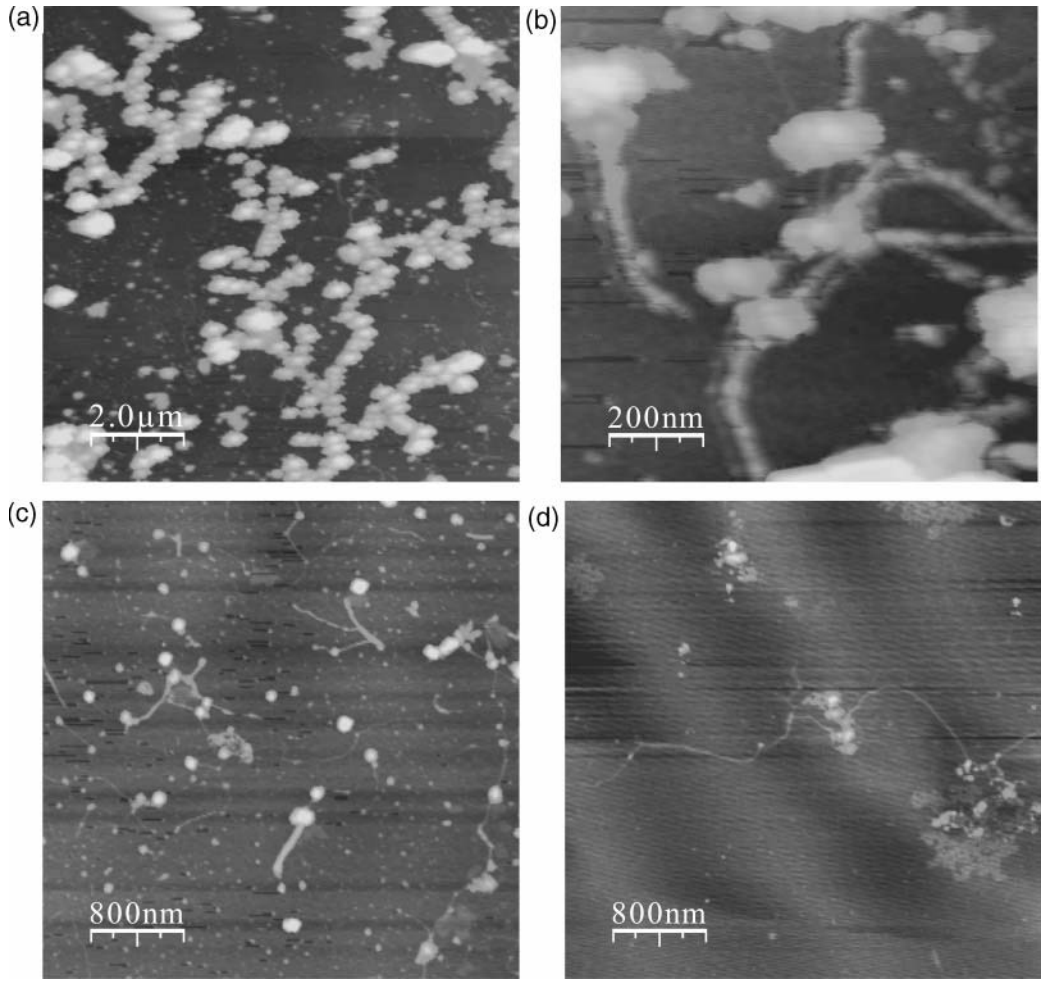

FIGURE 1. AFM images from samples taken from tributaries of the River Tame in the West Midlands, U.K. All samples were taken on April 8, 2003. (a) Sample taken from site 1; (b) enlarged view of the fibrils present in image A; (c) sample taken from site 2; (d) sample taken from site 3.

examining these data, it must be remembered that the AFM images a particular fraction of the aquatic colloids and may not always be representative of the whole sample. Further comparative studies between different techniques and different preparation methods on unperturbed samples, as have been performed previously (*32*−*34*), are still required as new methodologies are developed.

AFM Images. Representative images of River Tame and tributaries sampled in April and August, 2003 are presented in Figure 1 and also in the Supporting Information. As with previous analysis of this river at ambient, circumneutral pH values (*5*), the principal structures which were unambiguously visualized were the following: (1) fibrils of 1−10 nm in height (taken as a proxy for diameter) and greater than 100 nm in length; (2) globular material primarily in the range of 1−10 nm (in height), although in some cases up to 60 nm; (3) complete coverage by a surface film to a depth of ca. 10 nm. The surface coverage is discussed in a later section. These morphologies are completely different from those observed in a pristine stream fed by a glacier (*25*), where larger, near-spherical structures were observed (mean diameter ca. 30−70 nm). In addition, the glacier-fed stream showed a discrete or stacked platelet-type conformation, probably composed of silicate or carbonate (*25*), with very little material of obviously biological origin, reflecting the source of the colloids.

Despite the similarities of the visualized material with our previous work (*5*), a far greater range of structures were imaged, as the more extensive nature of the sampling campaign was able to more thoroughly detect the natural variability in the colloids conformation. In addition, networks of fibrils and intimate associations between fibrils and the roughly spherical material were observed. The images seen thus fit roughly within the structural classification scheme in the literature (*12*), which postulated small, inorganic spheres, small, roughly spherical humic substances, and fibrils as the three main types of colloids. However, while such a classification system is of immense importance allowing us to understand the structure and behavior of natural colloids, it will almost certainly underestimate the complexity of the natural system. This is the case with these samples. For instance, the networks of fibrils were often extensive and sometimes with cell debris incorporated within the network. In addition, the small, globular material is only very roughly spherical in most cases and shows a wide distribution of sizes, up to about 60 nm.

The pH of samples from sites 2 and 4, from the August sampling, was varied to both pH 4 and 10 by addition of dilute acid and base. The values were taken as extreme pH values, likely to give greatest conformational changes, but still relevant to natural water systems. Fewer discrete colloids were observed at both pH 4 and 10 compared with ambient pH. At pH 4, this perhaps reflects aggregation and loss of small colloids prior to sorption on the mica, due to the reduction in electrostatic repulsion at lower pH. At pH 10, this can also be provisionally explained by greater repulsive charge interaction between the mica and the colloids, again reducing sorption. Interestingly, at pH 4, colloid conformation

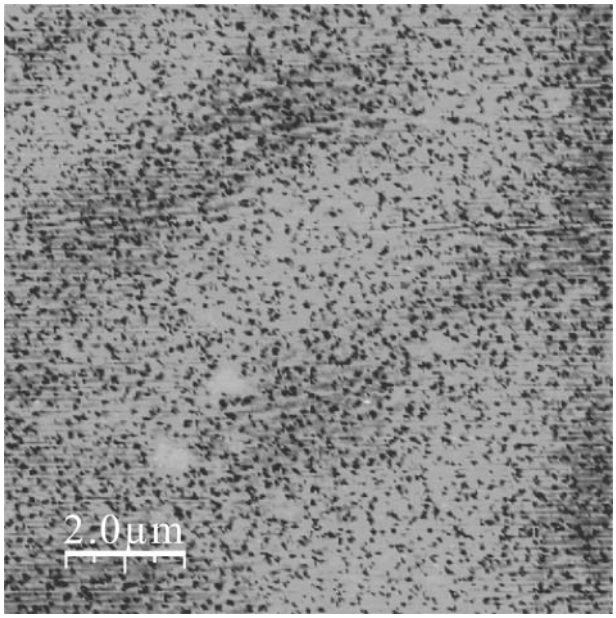

FIGURE 2. Representative AFM image from a sample taken from the River Tame, site 4, that has been altered to pH 10. The sample was taken and the pH altered on August 6, 2003. The lighter areas on the image indicate higher values (from the mica surface), the darker areas, thus, show pits within the surface layer.

generally resembles conformation at ambient pH. However, closer inspection of the images at pH 10 (Figure 2) reveals a completely different morphology, with an apparent surface film containing pits and a film with large spherical holes. We have interpreted this altered conformation as the growth of a surface film, although the reason for the pits is not clear. This conformation is only seen at pH 10 in a small number of samples.

Corrected Lateral Dimensions and Shape. Size distributions from AFM-derived heights and polydispersity values are presented in the Supporting Information. It is well-known that lateral dimensions significantly overestimate the size of small colloids, in particular, due to the radius of curvature of the tip being in the same range as the colloidal diameter. However, correction of the lateral dimensions can be performed if the radius of curvature of the tip is known, according to equations given in ref 18, although the corrections carry a degree of uncertainty and must be assessed with due caution. Ideal, new tips can be estimated at 10 nm, while older, but usable tips are approximately 50 nm. These are not measured values but assumptions to test the effect of the tip dimensions. We have used both sizes to correct for AFM overestimates and compared these corrected lateral dimensions with the AFM heights (Figure 3). As can be seen, under all conditions, the corrected lateral dimensions are substantially larger than the height values, indicating the flattened, near-spherical nature of the sorbed colloids (aspect ratio between 1.1 and 3, depending on the colloid and the

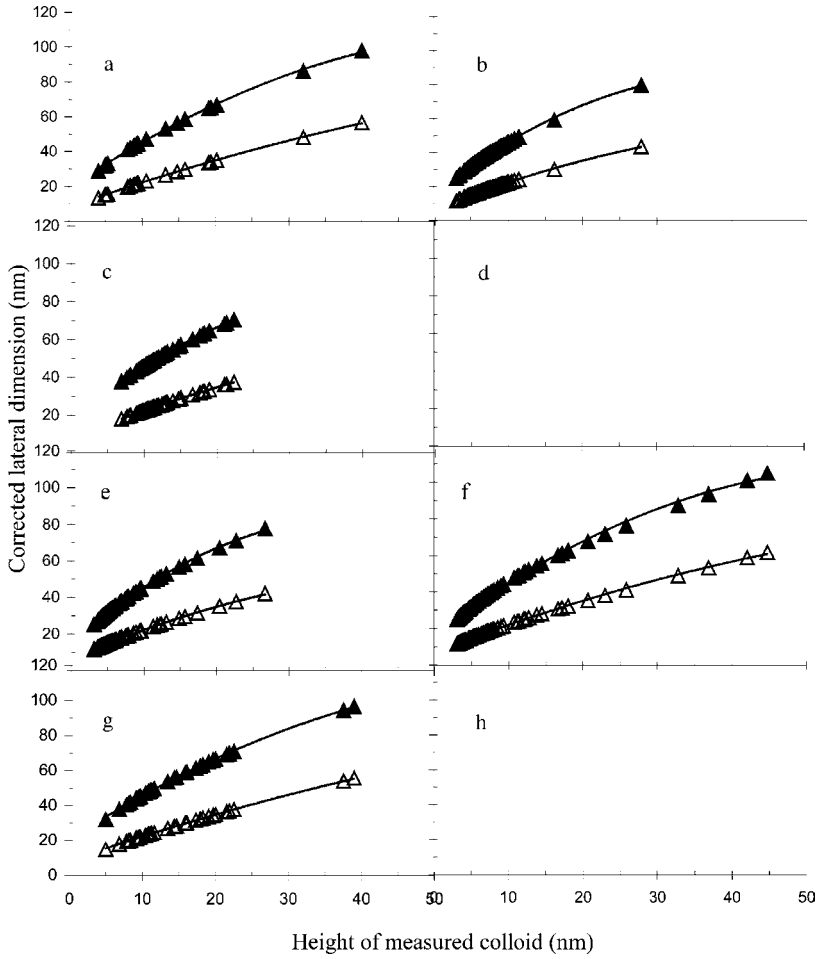

FIGURE 3. Corrected lateral dimensions for discrete particles measured in AFM images from samples taken from the River Tame and a tributary of the River Tame (▲ points assuming a 50 nm tip, △ points assuming a 10 nm tip). All samples were taken August 6, 2003. Due to the lack of any discrete particles in the images for sites 2 and 4 altered to pH 10, no graph could be produced for these sites. (a) Site 2, ambient conditions; (b) site 2, sedimented; (c) site 2, altered to pH 4; (d) site 2, altered to pH 10; (e) site 4, ambient conditions; (f) site 4, sedimented; (g) site 4, altered to pH 4; (h) site 4, altered to pH 10.

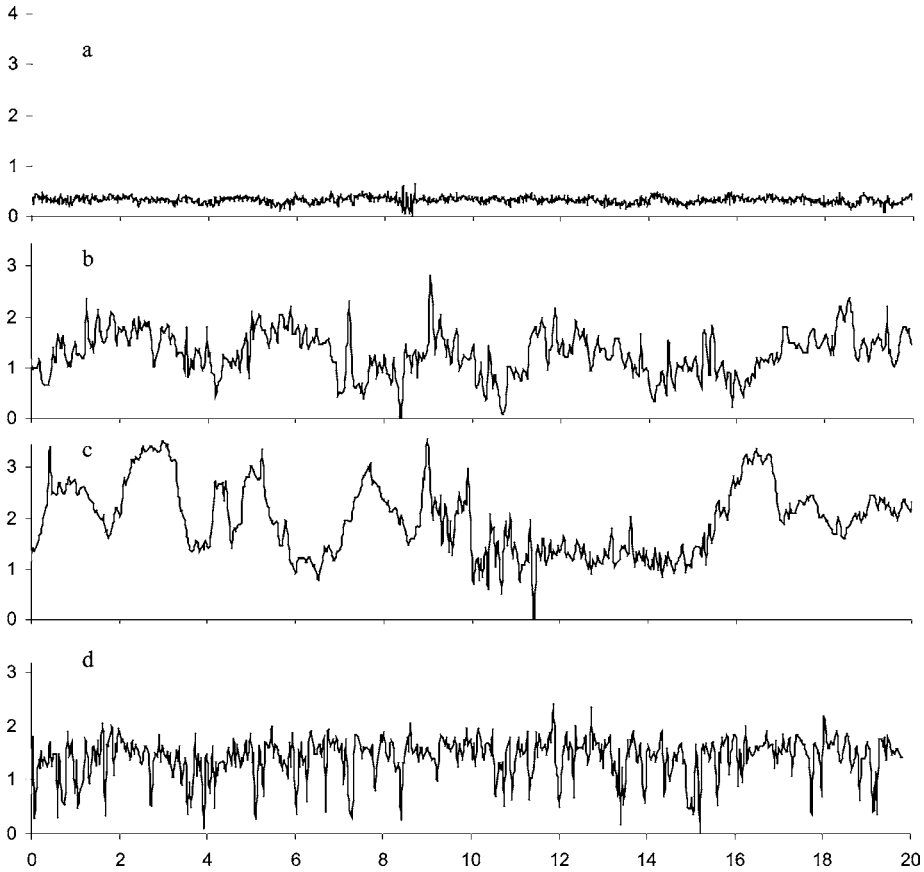

FIGURE 4. Graphs showing the surface coverage of mica in AFM images of samples taken from the River Tame, site 4, and for comparison, a graph of surface coverage on a piece of blank mica. (a) Blank mica; (b) sample from site 4; (c) sample from site 4 altered to pH 4; (d) sample from site 4 altered to pH 10.

TABLE 1. Calculation of Film Thickness and Sorbed Mass onto AFM Cantilevers[a]

cantilever no.	water sample	RF in air before immersion	RF in air after immersion	change in RF	spring constant	added mass (10^{-13} kg)	thickness *t*
1	whole	18807 ± 16	18082 ± 8	−725 ± 66	0.075	4.40	102
2	whole	19191 ± 6	19151 ± 7	−40 ±10	0.077	0.22	5
3	<1 μm	19312 ± 6	19107 ± 3	−205 ± 7	0.080	1.17	27
4	<1 μm	19268 ± 7	19036 ± 4	−232 ± 9	0.079	1.32	31
5	DI	17510 ± 8	17501 ± 12	−9 ± 14		nsc	nsc
6	DI	17481 ± 3	17479 ± 3	−2 ± 5		nsc	nsc

[a] RF, resonant frequency (Hz); spring constant in units of N m^{-1}; added mass in units of × 10^{-13} kg; thickness in nm; nsc, no significant change. "Whole" refers to unfractionated water (samples 1 and 2), <1 μm (samples 3 and 4) refers to nominal sizes estimated from SPLITT separation, and DI (samples 6 and 7) refers to deionized water. Spring constants are given in the text, with the exception of cantilever 5 (0.068 N m^{-1}) and cantilever 6 (0.059 N m^{-1}).

estimated tip size). This may be a reflection of their true shape in suspension but is also likely to be related to flattening on contact with the mica surface. This observation is nevertheless useful, as the behavior of small colloids sorbed to surfaces is important in understanding behavior at the solid−solution interface and the role of surface films in aggregation and pollutant partitioning (*35*).

Surface Coverage. Previously, coverage of clean surface such as mica or oxides of iron with adsorbed films of organic and possibly other colloidal material has been observed. Electrophoretic studies have shown that surface charge is dominated by this adsorbed layer in marine, estuarine, and freshwater environments (*36*, *37*), and more recent AFM experiments have indicated that force interactions between surfaces are dominated by this adsorbed layer (*22*). The surface film developed on exposure to natural waters or extracted HS is thus known to be important in surface-dominated processes such as aggregation and is a ubiquitous phenomena. However, most studies using either electrophoresis or AFM in force mode have investigated extracted humic substances (*23*, *24*, *38*), with consequent uncertainties about the effects on structure, and therefore surface sorption, due to the extraction process, which inevitably modifies the organic matter in the adsorbed layer. However, some studies have been performed on relatively unperturbed colloids (*22*). Indeed, here we demonstrate that a coherent surface film is developed on the mica at low, ambient levels of river water colloids and organic matter (Figure 4). However, coherent surface films only develop at high concentrations of (ca. 1000 mg L^{-1}) of extracted HS, while coverage is much lower at more realistic concentrations (*28*, *31*). Figure 4 shows AFM heights along a transect of a mica slide after exposure to distilled water and river water at various pH values. The mica exposed to distilled water is essentially flat on an atomic scale with variations in height of a few tenths of nanometers over several micrometers of length. However, after exposure

to river water, a substantially increased height variability of several nanometers was observed. This is a *minimum* height of the surface layer, as we do not know if the lowest height measured was of the mica or the adsorbed surface film, only that the AFM identifies a minimum point on any transect and calculates height from this. It is thus likely that the surface coverage is of greater depth than this. No variation of the surface layer thickness was observed as a function of pH, despite the difference in discrete colloids. However, at pH 10, it is evident that the frequency of height variations is greater, and this can be explained by the denser packing of the pits at high pH compared with the presence of the discrete particles at pH 7.5 and below, supporting our interpretation of Figure 2. The observed surface films have implications for our understanding of colloidal processes such as aggregation and surface film formation.

Thickness of the Surface Film. Table 1 reports the values of added mass and surface thickness calculated from data collected from resonance frequency changes on immersion of cantilevers in samples of river water. After immersion in distilled water no material was detected sorbed to the cantilever (samples 5 and 6), which confirms the data from Figure 4. However, upon immersion into river water, films of between 5 and 102 nm in thickness were developed, again confirming the data in Figure 4. For waters containing material nominally less than 1 μm in size, good agreement was given between replicates with an average film thickness of 29 nm developed (samples 3 and 4). For the unfractionated water sample (samples 1 and 2), a surface film certainly developed, confirming the results in Figure 4, but poor agreement between replicates was obtained (5 and 102 nm). The reason for this is unclear, but the heterogeneity and polydispersity of natural aquatic colloids would certainly contribute. For instance, the 102 nm film may have been based on the sorption of a small number of relatively high mass particles. In addition, the small surface areas and absolute values of mass measured would contribute to this variability, and repetition of these initial experiments with cantilevers with larger surface areas and resonant frequencies will be explored in the future to give more detailed information. These results give good agreement with Figure 4 and some quantification of the absolute thickness of the surface film which is not possible from the variability of the transects along the mica surface. In particular, the results indicate that surface films developed are unlikely to be composed of monolayers of very fine colloids (aquatic HS for instance is generally only a few nanometers in size (*18*, *19*)).

In conclusion, AFM has been shown to be a powerful tool for quantifying the structure of nanoscale natural aquatic colloids. Under ambient conditions, colloids from this temperate, urban river water fit roughly within the taxonomic classification of colloids in the literature (*12*), with a combination of fibrils and small, near-spherical colloids, often showing close attachment. In addition, the images observed generally contain very complex associations, sometimes with material which is likely to be cellular in origin based on morphology. Additionally, there was a ubiquitous presence of thin (<100 nm) surface films on mica and silicon nitride surfaces after exposure to river waters, indicating that pure, clean surfaces are unlikely to exist in real aquatic systems. The films are likely to have substantial effects on pollutant distribution between solid and solution and require further investigation.

Acknowledgments

We would like to acknowledge the Natural Environment Research Council (NER/M/S/2001/00073; NER/S/A/2000/03937) for funding this work.

Supporting Information Available

Methodology (calculations of number and weight-average heights) and results (Table S1, weight- and number-average heights and polydispersity index; Figure S1a−c, AFM images of River Tame; Figure S2a−h, particle size distributions of River Tame samples) are available. This material is available free of charge via the Internet at http://pubs.acs.org.

Literature Cited

(1) Buffle, J.; Van Leeuwen, H. P. *Environmental Particles*; Lewis Publishers: Boca Raton, FL, 1992; Vol. 1.
(2) Lead, J. R.; Davison, W.; Hamilton-Taylor, J.; Buffle, J. Characterizing colloidal material in natural waters. *Aquat. Geochem.* **1997**, *3*, 213−232.
(3) Gustafsson, O.; Gschwend, P. M. Aquatic colloids: concepts, definitions and current challenges. *Limnol. Oceanogr.* **1997**, *42*, 519−528.
(4) Stumm, W.; Morgan, J. J. *Aquatic Chemistry; Chemical Equilibria and Rates in Natural Waters*; John Wiley and Sons: New York, 1996.
(5) Muirhead, D.; Lead, J. R. Physicochemical characteristics of natural colloids in a heavily polluted, urban watershed: analysis by atomic force microscopy. *Hydrobiol.* **2003**, *494*, 65−69.
(6) Wilkinson, K. J.; Balnois, E.; Leppard, G. G.; Buffle, J. Characteristic features of the major components of freshwater colloidal organic matter revealed by transmission electron and atomic force microscopy. *Colloids Surf., A* **1999**, *155*, 287−310.
(7) Wilkinson, K. J.; Buffle, J. In *Physicochemical Kinetics and Transport at Biointerphases*; van Leeuwen, H. P., Koester, W., Eds.; John Wiley & Sons: Chichester, U.K., 2004.
(8) Wang, W. X.; Guo, L. D. Influences of natural colloids on metal bioavailability to two marine bivalves. *Environ. Sci. Technol.* **2000**, *34*, 4571−4576.
(9) Carvalho, R. A.; Benfield, M. C.; Santschi, P. H. Comparative bioaccumulation studies of colloidally complexed and free-ionic heavy metals in juvenile brown shrimp *Penaeus aztecus* (Crustacea: Decapoda: Penaeidae). *Limnol. Oceanogr.* **1999**, *44*, 403−424.
(10) Santschi, P. H.; Balnois, E.; Wilkinson, K. J.; Zhang, J.; Buffle, J.; Guo, L. Fibrillar polysaccharides in marine macromolecular organic matter as imaged by atomic force microscopy and transmission electron microscopy. *Limnol. Oceanogr.* **1998**, *43*, 896−908.
(11) Junta-Rosso, J. L.; Hochella, M. F.; Rimstadt, J. D. Linking microscopic and macroscopic data for heterogeneous reactions illustrated by the oxidation of manganese (II) at mineral surfaces. *Geochim. Cosmochim. Acta* **1997**, *61*, 149−159.
(12) Buffle, J.; Wilkinson, K. J.; Stoll, S.; Filella, M.; Zhang, J. A generalized description of aquatic colloidal interactions: The three-colloidal component approach. *Environ. Sci. Technol.* **1998**, *32*, 2887−2899.
(13) Leppard, G. G.; Arsenault, A. L. Note—Quantification of individual native biocolloids in natural waters: assessing indicators of aquatic events, by using transmission electron microscopy with a modified approach to image analysis. *Arch. Hydrobiol.* **2003**, *156*, 565−573.
(14) Redwood, P. S.; Lead, J. R.; Harrison, R. M.; Stoll, S. Characterization of humic substances by environmental scanning electron microscopy. *Environ. Sci. Technol.* **2005**, 39, 1962−1966.
(15) Doucet, F. J.; Lead, J. R.; Maguire, L.; Achterberg, E.; Millward, G. Visualisation of natural aquatic colloids and particles—a comparison of conventional high vacuum SEM and environmental scanning electron microscopy. *J. Environ. Monit.* **2005**, *7*, 115−121.
(16) Lead, J. R.; Wilkinson, K. J.; Starchev, K. Diffusion coefficients of humic substances in agarose gel and in water. *Environ. Sci. Technol.* **2003**, *37*, 482−487.
(17) Bouby, N.; Geckeis, H.; Manh, T. N.; Yun, J. I.; Dardenne, K.; Schafer, T.; Walther, C.; Kim, J. I. Laser-induced breakdown detection combined with asymmetrical flow field-flow fractionation: application to iron oxi/hydroxide colloid characterization. *J. Chromatog., A* **2004**, *1040*, 97−104.
(18) Balnois, E.; Wilkinson, K. J.; Lead, J. R.; Buffle, J. Atomic Force Microscopy of Humic Substances: Effects of pH and Ionic Strength. *Environ. Sci. Technol.* **1999**, *33*, 1311−1317.
(19) Maurice, P. A.; Namjesnik-Dejanovic, K. Aggregate structures of sorbed humic substances observed in aqueous solution. *Environ. Sci. Technol.* **1999**, *33*, 1538−1541.

(20) Plaschke, M.; Romer, J.; Kim, J. I. Characterization of Gorleben groundwater colloids by atomic force microscopy. *Environ. Sci. Technol.* **2002**, *36*, 4483−4488.
(21) Maurice, P. A.; McKnight, D. M.; Leff, L.; Fulghum, J. E.; Gooseff, M. Direct observation of aluminosilicate weathering in the hyporheic zone of an Antarctic dry valley stream. *Geochim. Cosmochim. Acta* **2002**, *66*, 1335−1347.
(22) Mosley, L. M.; Hunter, K. A.; Ducker, W. A. Forces between natural colloid particles in natural waters. *Environ. Sci. Technol.* **2003**, *37*, 3303−3308.
(23) Sander, S.; Mosley, L. M.; Hunter, K. A. Investigation of the interparticles forces in natural waters: effects of adsorbed humic acids on iron oxide and alumina surface properties. *Environ. Sci. Technol.* **2004**, *38*, 4791−4796.
(24) Assemi, S.; Hartley, P. G.; Scales, P. J.; Beckett, R. Investigation of adsorbed humic substances using atomic force microscopy. *Colloids Surf., A* **2004**, *248*, 17−23.
(25) Hannah, D. M.; Muirhead, D.; Lead, J. R. Imaging of suspended macromolecules and colloids in glacial and alpine streams by Atomic Force Microscopy. *J. Glaciol.* **2004**, *49*, 607−610.
(26) Davenport, A. J.; Gurnell, A. M.; Armitage, P. D. Habitat survey and classification of urban rivers. *River Res. Appl.* **2004**, *20*, 687−704.
(27) Chen, Y. W.; Buffle, J. Physicochemical and microbial preservation of colloid characteristics of natural water samples. I: Experimental conditions. *Water Res.* **1996**, *30*, 2178−2184.
(28) Balnois, E.; Wilkinson, K. J. Sample preparation techniques for the observation of environmental biopolmers by atomic force microscopy. *Colloids Surf., A.* **2002**, *207*, 229−242.
(29) Contado, C.; Blo, G.; Conato, C.; Dondi, F.; Beckett, R. Experimental approaches for size based metal speciation in rivers. *J. Environ. Monit.* **2003**, *5*, 845−851.
(30) Sader, J. E.; Larson, I.; Mulvaney, P.; White, L. R. Method for the calibration of atomic force microscope cantilevers. *Rev. Sci. Instrum.* **1995**, *66*, 3789−3798.
(31) Plaschke, M.; Romer, J.; Klenze, J.; Kim, J. In situ AFM study of sorbed humic acid colloids at different pH. *Colloids Surf., A.* **1999**, *160*, 269−279.
(32) Lead, J. R.; Balnois, E.; Hosse, M.; Menghetti, R.; Wilkinson, K. J. Characterizing colloidal material in natural waters. *Environ. Int.* **1999**, *25*, 245−258.
(33) Liss, S. N.; Droppo, I. E.; Flannigan, D. T.; Leppard, G. E. Floc architecture in wasterwater and natural riverine systems. *Environ. Sci. Technol.* **1996**, *30*, 680−686.
(34) Lead, J. R.; Wilkinson, K. J.; Balnois, E.; Cutak, B.; Larive, C.; Assemi, S.; Beckett, R. Diffusion coefficients and polydispersities of the Suwannee River fulvic acid: comparison of fluorescence correlation spectroscopy, pulsed-field gradient nuclear magnetic resonance and flow field-flow fractionation. *Environ. Sci. Technol.* **2000**, *34*, 3508−3513.
(35) Lyven, B.; Hassellov, M.; Turner, D. R.; Haraldsson, C.; Andersson, K. Competition between iron- and carbon-based colloidal carriers for trace metals in a freshwater assessed using flow field-flow fractionation coupled to ICP-MS. *Geochim. Cosmochim. Acta* **2003**, *67*, 3791−3802.
(36) Neihof, R. A.; Loeb, G. I. The surface charge of particulate matter in seawater. *Limnol. Oceanogr.* **1975**, *17*, 7−16.
(37) Hunter, K. A.; Liss, P. S. Organic matter and the surface charge of suspended particles in estuarine waters. *Limnol. Oceanogr.* **1982**, *27*, 322−335.
(38) Tipping, E.; Woof, C.; Cooke, D. Iron-Oxide from a seasonally anoxic lake. *Geochim. Cosmochim. Acta* **1981**, *45*, 1411−1419.

Received for review February 24, 2005. Revised manuscript received July 8, 2005. Accepted July 15, 2005.

ES050386J